Acta Scientific Neurology (ISSN: 2582-1121)

Volume 6 Issue 7 July 2023

Research Article

Functional Connectivity Difference for Navigation Ability

Greeshma Sharma[1]*, Ankita Gupta[2], Vijander Singh[3] and Sushil Chandra[4]

[1]*Neuro-XR Group, AI- Division, Centre for Development of Advanced Computing (CDAC)-Delhi, India*

[2]*Computer Science Department, Banasthali Vidyapith, Rajasthan, India*

[3]*Instrumentation and Control Engineering (ICE), Netaji Subhas University of Technology (NSUT), Delhi, India*

[4]*Biomedical Engineering Department, Institute of Nuclear Medicine and Allied Sciences (INMAS), DRDO-Delhi, India*

***Corresponding Author:** Greeshma Sharma, Neuro-XR Group, AI- Division, Centre for Development of Advanced Computing (CDAC)-Delhi, India.

Received: May 12, 2023

Published: June 26, 2023

Abstract

The present study examined the beta band electroencephalographic functional connectivity between various brain regions during different stages of spatial navigation: Planning of route, Navigation through a virtual maze, and Recall of travelled path, for navigators classified as good or bad. Coherence was used to compute functional connectivity. A graph theoretical analysis was used to quantify the organizational features of functional networks at each stage in order to identify key topological differences due to different stages or individual differences. The results reveal a reduction in the indices of modularity and small worldness during Navigation in comparison to the indices at Rest and the radius was significantly higher during Planning as compared to Navigation and Recall. Additionally, the highest degree and transitivity were observed for good navigators as compared to higher the global efficiency for poor navigators. Altogether, these results suggest that different stages of a spatial navigation task as well as differences in navigational abilities induce significant changes in the functional connectivity, that can be measured using coherence and graph theoretical analyses.

Keywords: Functional; Connectivity; Navigation

Introduction

This study computed functional connectivity [1] in the beta frequency band of EEG data during different stages of spatial navigation: Planning of tentative route, Navigation through a virtual maze, and Recall of the path taken. Numerous studies have revealed a parallel mode of activity in multiple cortical areas during a large array of cognitive processes [2-6]. Pursuing similar lines of thought, it can be assumed that vast changes in information flow will occur between different stages of spatial navigation (Planning, Navigation and Recall) since they present different objectives and consequently entail varying levels of cognitive effort from the subjects. In order to explore this assumption, we investigated the changes in functional connectivity of EEG channels between stages.

Functional connectivity networks are implicated in cognitive functioning [7] and may form the physiological basis of information processing and mental representations [8]. Subsequently, the topological architecture of these functional connectivity networks was quantified using several well-defined graph theory metrics. Coherence [9] was used to compute functional connectivity in the beta band between all pair-wise combinations of EEG channels. It has been used as a functional connectivity measure in many research

fields, including physiology [10], neurological disorders [11] and exercise physiology [12]. Coherence [9] was used to compute functional connectivity in beta band between all pair-wise combinations of EEG channels. Coherence is defined as the measure of synchronization between two brain regions in terms of spectral density. The current study applied a nonparametric approach: MATLAB's 'mscohere' algorithm which is based on Welch's averaged modified periodogram method [13]. The Welch estimator can be computed by Fast Fourier Transform (FFT) and is commonly used in spectral estimation. Understanding the propagation of EEG signals is essential in order to determine the information flow between brain regions and the level of their connectivity.

The theta and gamma band activity during spatial navigation and retrieval have been explored quite extensively [14-18], however, the potential functional role of beta band oscillations during the same is not yet fully understood [19-21]. Low amplitude beta waves with multiple and varying frequencies are often associated with active, busy or anxious thinking and active concentration [22]. In an attempt to correlate varying levels of cognitive processing with individual differences in navigation abilities we have examined the beta band activity.

The novelty of the present study in the context of existing literature resides in the integration of 64-channel EEG, Oculus Rift and Graph Theory to explore the individual differences in spatial navigation abilities.

Materials and Method

Participants

Electroencephalographic data was obtained from 30 healthy, right-handed subjects (25 males and 5 females) with normal or corrected-to-normal vision. Informed consent was obtained in writing and the research protocol was approved by the Institute of Nuclear Medicine and Allied Sciences (INMAS).

Classification

In order to rate the navigational abilities of the participants the Santa Barbara Sense of Direction (SODS) scale [23] was used. Each participant received a score between 1 and 7, with the higher the score, the better the perceived sense of direction.

EEG data acquisition

Continuous EEG data were recorded using the 'eego™' sports amplifier at a frequency range of 0.2-70Hz with 64 Ag/AgCl electrodes on the head-cap in accordance with the 10-20 electrode system. The ground electrode was positioned 10% anterior to FZ (AFz), with linked earlobes serving as references. Connectivity on all electrodes was ensured and impedance at all electrodes was minimized to below 5kΩ. The amplifier parameters were set as follows: input impedance ≥1GOhm, maximum sampling rate = 1024Hz, sensitivity = 6000 microV/cm, and CMRR ≥100dB.

Virtual maze

For this experiment, the participants were required to navigate through a brick wall virtual maze of area 282*362 units programmed in Unity 3D. A wireless joystick was used to manoeuvre movement inside the environment. The VM was displayed on the Oculus Rift DK2 through MacBook Air, 13-inch screen, processor 1.4 GHz core i5 with a resolution of 1920x1200 pixels (Figure 1).

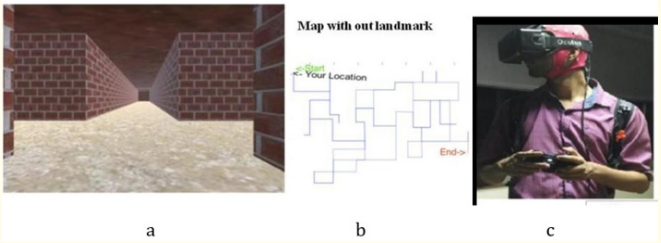

Figure 1: a) Virtual Maze navigation. b) Map for planning navigation from start to end point. c) Subject wearing device and navigating in the environment.

Experimental design and procedure

Prior to the experiment the participants were familiarized with the immersive experience and controls of the system. The participants were instructed to navigate a virtual maze (VM) after planning the route and reach the end destination marked by green object.

The experiment procedure involved continuous recording the EEG signals of the subjects during the following four stages of the task

- **Baseline (Rest):** Subjects were seated in a relaxed position with no active task.
- **Planning:** Subjects were shown a map of the VM to plan a tentative route so that they could exit the VM in minimum time.
- **Navigation:** Subjects had to reach destination by travelling into VM.
- **Recall:** On exiting the maze subjects had to draw the path they had actually taken on a piece of paper.

The start and the end time (and hence duration) of each of the four stages was recorded using a time stamp mechanism embedded in the game.

Behaviour measures

The Unity software automatically measured participant's position in x–y coordinates and heading orientation (yaw). These data were automatically output into a text file and converted by custom software that plotted the navigation path onto a 2D map of the space. The software then calculated performance score. Performance score included coordinates of the path traveled by the participants, proportions of repetitions, total time taken for navigation, average number of map views, average time spent to view a map, number of turns, and total distance covered. 'Proportions of repetitions' was defined as the ratio of a total number of repetitions of the path and the sum of repetitions and non-repetitions of the path. 'Average time spent to view a map' was an average time spent by the participants to view the map. 'Average number of map views' was defined an average number of times map was viewed during way finding from the start-point to the end-point. 'Total time taken for navigation was the time taken from the start-point to the end-point. Maximum allotted total time was 15 min; but, if participants failed to reach the end-point within this time, then the VM automatically disappeared. 'Number of turns' was defined as the total number of turns taken by participants during way finding.

EEG signal processing

Baseline noise was removed using EEGLAB [24]. Independent Component Analysis (ICA) was used to reject artifacts. A notch filter was used to remove the artifacts due to the line frequency (50Hz). The preprocessed data was converted to a standard matrix in MATLAB, which was then separated into each stage of the experiment with the help of sampling frequencies and time stamps for the start and end of each stage. The beta-band data was extracted from each segment by using the discrete wavelet transform (db4) and fifth-order decomposition implemented via MATLAB commands "wavedec" and "wrcoef."

Graph Theoretical analysis

Estimation of functional connectivity and Association matrix

Coherence is used to measure task related functional interactions between brain regions [9]. It is an estimate of the consistency of the relative amplitude and phase between signals detected at electrodes within a set frequency band. It is a normalized quantity bounded by 0 and 1 (zero implying linear uncorrelation and one implying maximum linear correlation). Coherence between all pairwise combinations of EEG channels was conventionally represented in a 64×64 association matrix A = aij where each matrix entry aij represents the connection between node i and node j ($1 \leq i, j \leq 64$). Following a commonly undertaken practice to eliminate likely false-positives, an arbitrary threshold of 30% was applied to eliminate 70% of the weakest connections (Figure 2).

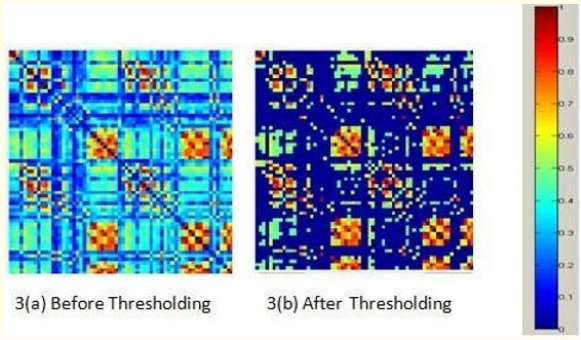

Figure 2: a) Association Matrix before thresholding showing all of the functional connections as evaluated by Coherence. B) Association Matrix after 30% thresholding showing the strongest 30% connections only (the weakest 70% connections have been eliminated).

Network measures and network visualization

The network topologies were characterized using several graph theory metrics calculated from the EEGNET toolbox [25]. A network is a mathematical representation of a real-world complex system and is defined by a collection of nodes (vertices) and links (edges) between pairs of nodes. The diameter of graph is the maxi-

mum distance between the pair of vertices. A radius of the graph exists only if it has the diameter. The minimum among all the maximum distances between a vertex to all other vertices is considered as the radius of the Graph. normalized network density (or cost) as a total number of edges in the graph, divided by the maximum possible number of edges. The degree is one of the most common measures of centrality. Nodes with a high degree are interacting, structurally or functionally, with many other nodes in the network. Characteristic path length (CPL) of the network is the average shortest path length between all pairs of nodes in the network and is the most commonly used measure of functional integration. The average inverse shortest path length is a related measure known as global efficiency. The degree to which the network may be subdivided into such clearly delineated and no overlapping groups is quantified by a single statistic, modularity. A classical variant of the clustering coefficient, known as the transitivity, is normalized collectively. Small-world networks are formally defined as networks that are significantly more clustered than random networks yet have approximately the same characteristic path length as random networks. The detailed formula and definitions of the measures can be found in a paper of basic graph theory [8].

Results

Median split classification was applied on scores of SODS and participants were classified accordingly (median = 4.5, Good Navigator = 12, Bad navigator = 18). Multivariate ANOVA showed non-significant differences between behavioral outcomes of participants recorded in the virtual maze, F (1,25) = 1.23, p>.05. Good navigators exited the maze in relatively lesser time and committed fewer errors than the poor navigators (Table 1).

Behaviuoral indicators	Good navigator		Bad navigator	
	Mean	S.D.	Mean	S.D.
Properties of repetition	0.220857	0.179313	0.2106	0.146084
Areas visited once	23.14286	3.907084	25.4	4.694678
Repetitions	5.833333	5.2095	8.8	7.560423
Max time(min)	12.85714	5.248907	15	0
Time taken (sec)	362.1429	218.81	362.4	146.2335
Planning time(sec)	51.85714	20.63581	77.1	41.28062
No. of times map used	38.71429	26.47756	26.5	13.53699
Map viewing time (sec)	94.42857	71.08718	83.7	44.94897
Total time	414	238.0336	879	1346.026
Navigation time?	6.428571	3.849198	6.1	2.118962
No. of turns?	14.42857	5.924698	18.1	9.126336

Table 1: Behavioral Parameters.

Stages	Subjects		CPL	Global Efficiency	Radius	Diameter	Highest Degree	Density	Number of Nodes	Small world Coefficient	Number of Edges	Modularity	Transitivity
Baseline	Good	Mean	1.88	0.54	2.43	4.86	36	0.3	64	0.13	602.14	0.33	0.46
		S.D.	0.26	0.08	0.73	1.36	1.41	0	0	0.14	4.22	0.07	0.17
	Bad	Mean	1.89	0.61	2.5	4.5	34.1	0.3	64	0.25	598.4	0.34	0.3
		S.D.	0.13	0.04	0.67	1.02	1.58	0	0	0.13	4.78	0.07	0.13
Navigation	Good	Mean	1.86	0.53	2.43	4.57	37.43	0.3	64	0.09	606.14	0.29	0.5
		S.D.	0.15	0.06	0.49	0.49	2.44	0	0	0.1	6.01	0.08	0.11
	Bad	Mean	1.83	0.58	2.4	4.1	33.9	0.3	64	0.15	602.2	0.3	0.34
		S.D.	0.13	0.07	0.49	0.54	2.26	0	0	0.18	6.05	0.05	0.1
Planning	Good	Mean	2.02	0.55	3.14	5.29	39	0.3	64	0.13	602.29	0.31	0.46
		S.D.	0.21	0.06	0.64	0.88	2.73	0	0	0.08	6.47	0.07	0.11
	Bad	Mean	1.91	0.57	2.7	4.7	35.3	0.3	64	0.15	602.1	0.29	0.35
		S.D.	0.14	0.07	0.46	0.64	3.35	0	0	0.13	4.46	0.09	0.1
Recall	Good	Mean	1.87	0.51	2.14	5.14	37.71	0.3	64	0.06	601	0.3	0.55
		S.D.	0.23	0.08	0.35	1.55	1.98	0	0	0.11	4.93	0.11	0.16
	Bad	Mean	1.91	0.6	2.6	4.3	33.7	0.3	64	0.11	599.1	0.35	0.35
		S.D.	0.14	0.03	0.49	0.46	3.41	0	0	0.21	6.28	0.07	0.14

Table 2: Graph Theory Parameters.

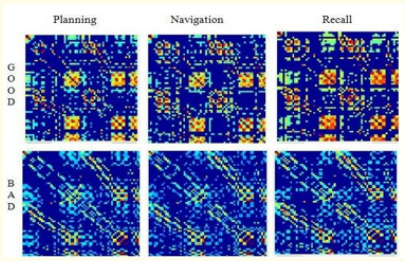

Figure 3: Strong intra-network connectivity profiles were observed for good navigators as opposed to poor navigators in all the three task stages. Note the appearance of more cluttered brighter pixels in case of good navigators.

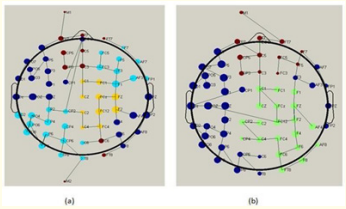

Figure 4: Mean Brain Network of all the participants during (a) Baseline and (b) Navigation. The color varying parameter of the nodes is 'Module'. All nodes belonging to one Module are of the same color. As is evident from the figures, the brain network during Baseline is more Modular (i.e., having greater number of modules) than the brain network during Navigation.

Figure 5: a) Mean Transitivity and b) Mean highest degree. Good navigators have higher transitivity and degree compared to bad navigators.

Results showed strong intra-network connectivity profiles for good navigators as opposed to poor navigators (Figure 3). All network measures are summarized in the Table 2. Univariate ANOVA on the graph parameters showed significant differences in Radius between three stages: Planning, Navigation, and Recall, F (2,22) = 4.303, p<.01. The radius was higher during Planning than that during Navigation and Recall. Paired sample t-test was applied on the graph measures between all the stages taken pairwise at a time. It was found that both modularity and small world index decreased during Navigation in comparison to the indices during Baseline. In good navigators, modularity, t (11) = 2.352, p<.05, Small world index, t (11) = 2.46, p<.05 had shown significant differences; whereas in bad navigators, modularity, t (17) = 2.512, p<.05, small world index, t (17) = 2.656, p<.05, had shown significant differences (Figure 4). Also, the good navigators had higher transitivity and degree than their counterparts. Between group analysis revealed, significant highest degree, F (1,25) = 8.303, p<.05, and transitivity, F (1,25) = 7.790, p<.05in good navigators (Figure 5).

Discussion

In the present study, we analyzed functional connectivity networks during Planning, Navigation, and Recall stages, taking into account individual differences in navigation ability. Beta band was chosen to be explored further because of its relevance and limited exploration in navigation. Since association matrices by themselves were not sufficient to assess the dynamic changes in brain network interactions, we employed graph theory to elucidate quantifiable differences in functional networks. Results revealed that the mean highest degree of good navigators was significantly higher than that of bad navigators, implying greater centrality and influence over the network as compared to the networks of bad navigators. Moreover, the mean transitivity was also higher in the case of good navigators as compared to bad navigators. Higher transitivity in good navigators suggests a proclivity towards segregated neural processing, i.e., a preference to be arranged in clusters or densely and mutually interconnected neighborhoods. At this point, it is compelling to mention that although the widely used index of global efficiency failed to significantly differentiate between good and bad navigators, its value for good navigators was consistently lower than that for bad navigators throughout all the stages. The trend in bad navigators toward more globally efficient networks may appear counter-intuitive. The positive relationship between cognitive load and global integration [26], on the other hand, supported the theory that greater cognitive load experienced by poor navigators resulted in a reorganization of their brain networks towards a more globally integrated pattern. When combined with

increased transitivity in good navigators, higher global efficiency in bad navigators reinforced the fact that good navigators' brain networks prioritize local connectedness over global connectedness.

It is critical to investigate the reason for good navigators' lower cognitive load while navigating. The competency of a good navigator lies in the fact that they can switch flexibly between different strategies, choosing the most optimal alternative in accordance with task demands. Naturally, different strategies and approaches impose different levels of cognitive load, and good navigators are subject to lesser cognitive loads as a consequence of optimal strategy selection and utilization of brain resources. In a direct contrast, navigators with unsatisfactory levels of competency are more rigid in their approach, leading to a higher cognitive load. In support of our argument, evidence has been found that individuals systematically differ in their processing capacity. When comparing the three stages, Radius was found to be significantly higher in the Planning stage as compared to the Navigation and Recall stages. Keeping in mind that a disconnected graph has an infinite radius, we infer that the brain networks were better connected in Navigation and Recall stages than the networks in planning stage. This could be because navigation and recall are more cognitively demanding than planning, and as cognitive effort increases, the brain functional network reorganizes towards a more globally integrated pattern [26]. When the parameters corresponding to the rest and navigation stages were compared, the indices of modularity and small worldness were found to be lower during navigation than during rest. Navigation entailed higher cognitive efforts than Rest and the diminishing index of modularity in response to enhanced cognitive load reflects the propensity of the brain to reorganize itself into a less modular network. In addition, from the perspective of small-world architecture, the economically configured brain at rest had adopted an expensive and less efficient architecture in response to increasing cognitive demands. Our findings were in accordance with a previous study that reported a negative correlation between task difficulty, brain modularity, and the cost-effectiveness of the network [5,26].

Conclusion

In conclusion, our findings show that graph theoretical methods can be used to obtain quantifiable estimates of brain connectivity differences owing to varying navigation abilities in individuals. Additionally, between- stage analyses elucidated the manner in which the brain manifests reorganization in response to enhanced cognitive load. Our results show that the brain networks of people with a good sense of direction have a higher propensity to organize themselves into clusters and communities, whereas the brain networks of people with a poor sense of direction tend to be globally integrated owing to a higher cognitive load. Furthermore, our results substantiate a previous study that reported a shift toward a less modular, more globally integrated, and more expensive network in response to enhanced cognitive load. These results suggest that local connectivity could be an effective target of assistive interventions for deficits in navigation. Strengthening or selective modulation of local connectivity might help to remediate difficulties in navigation and route learning mechanisms.

Sources of Funding

This research did not receive any grant from any funding institutions in the public or private sector.

Conflict of Interest

The author has no conflict of interest to declare.

Bibliography

1. Lang EW., *et al*. "Brain Connectivity Analysis: A Short Survey". *Computational Intelligence and Neuroscience* (2012): 1-21.

2. Başar E., *et al*. "Gamma, alpha, delta, and theta oscillations govern cognitive processes". *International Journal of Psychophysiology* 39.2-3 (2001): 241-248.

3. Engel AK and Singer W. "Temporal binding and the neural correlates of sensory awareness". *Trends in Cognitive Sciences* 5.1 (2001): 16-25.

4. Gevins A. "High-resolution EEG mapping of cortical activation related to working memory: effects of task difficulty, type of processing, and practice". *Cerebral Cortex* 7.4 (1997): 374-385.

5. Vecchio F., *et al*. "Inter-hemispherical functional coupling of EEG rhythms during the perception of facial emotional expressions". *Clinical Neurophysiology* 124.2 (2013): 263-272.

6. Wyczesany M., *et al*. "Cortical functional connectivity is associated with the valence of affective states". *Brain and Cognition* 90 (2014): 109-115.

7. Varela F., *et al*. "The brainweb: Phase synchronization and large- scale integration". *Nature Reviews Neuroscience* 2.4 (2001): 229-239.

8. Bullmore E and Sporns O. "Complex brain networks: graph theoretical analysis of structural and functional systems". *Nature Reviews Neuroscience* 10.3 (2009): 186-198.

9. Bendat JS and Piersol AG. "Random Data: Analysis and Measurement Procedures, 4th Edition". John Wiley and Sons (2010): 640.

10. Cantero JL., *et al*. "Alpha EEG coherence in different brain states: an electrophysiological index of the arousal level in human subjects". *Neuroscience Letters* 271.3 (1999): 167-170.

11. Adler G., *et al*. "EEG coherence in Alzheimer?s dementia". *Journal of Neural Transmission* 110.9 (2003): 1051-1058.

12. Deeny SP., *et al*. "Cortico-cortical Communication and Superior Performance in Skilled Marksmen: An EEG Coherence Analysis". *Journal of Sport and Exercise Psychology* 25.2 (2003): 188-204.

13. Welch P. "The use of fast Fourier transform for the estimation of power spectra: A method based on time averaging over short, modified periodograms". *IEEE Transactions on Audio and Electroacoustics* 15.2 (1967): 70-73.

14. Bischof WF and Boulanger P. "Spatial Navigation in Virtual Reality Environments: An EEG Analysis". *CyberPsychology and Behavior* 6.5 (2003): 487-495.

15. Duarte IC., *et al*. "The anterior versus posterior hippocampal oscillations debate in human spatial navigation: evidence from an electrocorticographic case study". *Brain and Behavior* 6.9 (2016): e00507.

16. Kahana MJ., *et al*. "Human theta oscillations exhibit task dependence during virtual maze navigation". *Nature* 399.6738 (1999): 781-784.

17. White DJ., *et al*. "Brain Oscillatory Activity during Spatial Navigation: Theta and Gamma Activity Link Medial Temporal and Parietal Regions". *Journal of Cognitive Neuroscience* 24.3 (2012): 686-697.

18. Sederberg PB., *et al*. "Theta and Gamma Oscillations during Encoding Predict Subsequent Recall". *The Journal of Neuroscience* 23.34 (2003): 10809-10814.

19. Liu J., *et al*. "Redesigning navigational aids using virtual global landmarks to improve spatial knowledge retrieval". *NPJ Science of Learning* 7.1 (2022): 17.

20. Huong NTM., *et al*. "Classification of Left/Right Hand Movement EEG Signals Using Event Related Potentials and Advanced Features" (2018): 209-215.

21. Velasco-Álvarez F., *et al*. "Audio-cued motor imagery- based brain-computer interface: Navigation through virtual and real environments". *Neurocomputing* 121 (2013): 89-98.

22. Baumeister J., *et al*. "Influence of phosphatidylserine on cognitive performance and cortical activity after induced stress". *Nutritional Neuroscience* 11.3 (2008): 103-110.

23. Hegarty M. "Development of a self-report measure of environmental spatial ability". *Intelligence* 30.5 (2002): 425-447.

24. Delorme A and Makeig S. "EEGLAB: an open source toolbox for analysis of single-trial EEG dynamics including independent component analysis". *Journal of Neuroscience Methods* 134.1 (2004): 9-21.

25. Hassan M., *et al*. "EEGNET: An Open Source Tool for Analyzing and Visualizing M/EEG Connectome". *PLoS One* 10.9 (2015): e0138297.

26. Vatansever D., *et al*. "Default Mode Dynamics for Global Functional Integration". *Journal of Neuroscience* 35.46 (2015): 15254-15262.